Synthesis and Crystal Structures of S_2O_2 Macrocycle L, and its Silver(I) and Platinum(II) Complexes (Where L = 5,8-dioxa-2,11-dithia-[12]-*o*-cyclophane)

IL YOON[1], KI-MIN PARK[1], JONG HWA JUNG[1]*, JINEUN KIM[1], SUNG BAE PARK[2] and SHIM SUNG LEE[1]**

[1]*Department of Chemistry and Research Institute of Natural Sciences, Gyeongsang National University, Chinju 660-701, S. Korea;* [2]*Department of Chemistry, Inje University, Kimhae 621-749, S. Korea*

Abstract

The S_2O_2-donor macrocycle, **L** (5,8-dioxa-2,11-dithia-[12]-*o*-cyclophane or 3,4-benzo-1,6-dithia-9,12-dioxocyclo-tetradecane-3-ene) was synthesized by ring closure reaction of 2,2′-(ethylenedioxy)diethanethiol with α,α'-dibromo-*o*-xylene under high dilution and crystallized from methanol. The X-ray structure of **L** has a C_2 axis and is shown to have two S atoms oriented *exodentate* and two O atoms positioned *endodentate* to the ring cavity. Reaction of $AgNO_3$ with **L** affords monomeric [Ag(**L**)(NO$_3$)], (**1**) in which the Ag atom is in a distorted trigonal plane coordinated by two S atoms in a ring and to one O atom from the NO_3^- ion. The behavior of complex **1** in solution was also characterized by NMR titration. Reaction between K_2PtCl_4 and **L** affords [Pt(**L**)Cl$_2$], (**2**) in which the Pt atom has a distorted square-planar environment, coordinated to two S atoms of **L** and to two Cl$^-$ ions in a *cis* arrangement.

Introduction

Recently the synergistic effect of the thiaoxa-donor macrocycles on the coordination properties of metallic complexes caused by replacement of one or more S donors from homoleptic thiacrown ethers has been apparent in the literature [1–5]. Thiaoxa macrocycles in particular have received considerable attention due not only to their role as a connection between crown ethers and thiacrown ethers, but also their ability to discriminate between metal ions in separation, detection and structural chemistry [1–11].

In fact, some S_2O-donor macrocycles based on a monobenzo subunit have been shown to be excellent sensors in Ag(I)-selective membrane electrodes [6–8]. According to our preliminary work [10], **L**, an *ortho*-type S_2O_2-donor macrocycle was found to be the most effective Ag(I) extractant among its isomers, while the *para*-type isomer exhibited the lowest extractability. Since little is known about the metal complexes for **L** except for the Pd(II) complex [11], the coordination properties based on crystal structures of the complexes of **L** with soft metals or platinum group metals became our recent interest.

As a part of our continuing interest in the coordination properties of both cyclic and acyclic thiaoxa ligands [9-12], we report herein the results of our investigation on the pre-paration and crystal structures of **L** and its coordination to metal ions, in particular Ag(I) and Pt(II).

L
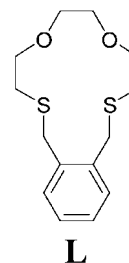
Experimental

Materials for synthesis

The 2,2′-(ethylenedioxy)diethanethiol and α, α'-dibromo-*o*-xylene were purchased from Aldrich and used as received. Thin-layer chromatography was carried out on plates coated with Merck silica UV-254. For flash column chromatography, Merck silica gel 60 (No. 9385, 230-400 mesh) was used.

Analytical procedures

^{1}H and ^{13}C{^{1}H} NMR spectra were recorded on a Bruker DRX-500 spectrometer operating at 500 and 125.7 MHz, respectively. Infrared spectra were measured with a Mattson Genesis Series FT-IR spectrophotometer. Microanalyses were performed by Elemental Analysen Systeme Vario EL

and mass spectra were obtained on a Kratos Profile HV-3 spectrometer at the Korea Basic Science Institute. Melting points are uncorrected.

Preparation of 5,8-dioxa-2,11-dithia[12]-o-cyclophane, **L**

KOH (2.10 g, 37.5 mmol) was dissolved in ethanol (1000 mL) in a 3L round-bottom flask. A solution of 2,2′-(ethylenedioxy)diethanethiol (2.73 g, 15.0 mmol) and α, α'-dibromo-*o*-xylene (3.96 g, 15.0 mmole) in ethanol (30 mL) was drawn into a 50-mL glass syringe. Under nitrogen atmosphere, the solution was added dropwise to the refluxing solution at a rate of 0.6 mL h^{-1} with a microprocessor controlled syringe pump during a 50-h period. The mixture was refluxed for another 10 h. After cooling to room temperature the reaction mixture was filtered and evaporated. Water (100 mL) was added to the residue and the mixture was extracted with dichloromethane (3 × 70 mL). The combined organic layers were dried over anhydrous sodium sulfate and evaporated to give a yellow oil. The product was recrystallized from diethyl ether to give **L** as a white solid (1.01 g, 37%). Sublimation under vacuum (10^{-2} torr or lower, 95–100 °C) gave a white solid. Colorless crystals suitable for X-ray crystallography were grown by slow evaporation from methanol. δ_H (CDCl$_3$, 500 MHz) 7.18–7.35 (4H, m, aromatic), 4.19 (4H, s, SCH_2Ph), 3.81 (4H, t, J 5.0 Hz, OCH_2CH$_2$S), 3.69 (4H, s, OCH$_2$CH_2O), 2.71 (4H, t, J 5.0 Hz, OCH$_2$CH_2S); δ_C (CDCl$_3$, 125 MHz) 136.91, 130.60, 127.52, 73.35, 70.22, 35.29, 32.50; IR (KBr): 3061, 2906, 2865, 2361, 1113, and 767 cm^{-1}. M.p. 110–112 °C. Mass spectrum *m/z* 284 (M, 36%), 224 (23), 162 (82), 135 (100), 134 (55), 104 (81), 91 (42). Anal. Calcd for C$_{14}$H$_{20}$O$_2$S$_2$: C, 59.12; H, 7.09; S, 22.55%. Found: C, 59.27; H, 6.82; S, 22.52%.

*Preparation of [Ag(**L**)(NO$_3$)],* **1**

AgNO$_3$ (0.030 g, 0.176 mmol) was dissolved in methanol (5 mL) and was added to the solution of **L** (0.050 g, 0.176 mmol) in methanol (5 mL). The reaction mixture was stirred in the dark for 1 h and filtered. Slow evaporation of the filtrate in the dark produced colorless crystals of the product which were suitable for X-ray crystallography. IR (KBr) 3061, 2097, 2869, 2352, 1355 (NO$_3^-$), 1105 and 769 cm^{-1}. Yield ca 80%. Decomp. 173–174 °C. Anal. Calcd for C$_{14}$H$_{20}$AgNO$_5$S$_2$Ag: C, 37.01; H, 4.44; N, 3.08; S, 14.12. Found: C, 37.35; H, 4.13; N, 3.19; S, 14.11%. FAB mass spectrum: *m/z* = 391 [^{107}Ag**L**]$^+$, 393 [^{109}Ag**L**]$^+$.

*Preparation of [Pt(**L**)Cl$_2$],* **2**

Complex **2** was prepared by the reaction of equimolar amounts of **L** and K$_2$PtCl$_4$ in water/dichloromethane. The yellow precipitate that formed immediately was filtered, recrystallized from acetonitrile by slow evaporation to give reddish yellow single crystals suitable for X-ray analysis. IR (KBr) 3009, 2889, 2854, 2357, 2332, 1137 and 761 cm^{-1}. Yield ca 50%. Decomp. 225–227 °C. Anal. Calcd for C$_{14}$H$_{20}$PtO$_2$S$_2$Cl$_2$Ag: C, 30.55; H, 3.66; S, 11.65%. Found: C, 30.61; H, 3.67; S, 11.56%. FAB mass spectrum: *m/z* = 515 [^{195}Pt(**L**)Cl]$^+$.

X-ray data collection, structure determination and refinement

Crystals suitable for X-ray diffraction were mounted on a Siemens SMART diffractometer equipped with a graphite monochromated Mo$K\alpha$ (λ = 0.71073 Å) radiation source and a CCD detector and 45 frames of two-dimensional diffraction images were collected and processed to deduce the cell parameter and orientation matrix. A total of 1271 frames of two-dimensional diffraction images were collected, each of which was measured for 30 sec. The frame data were processed to give structure factors by the program SAINT [13]. The intensity data were corrected for Lorentz and polarization effects. Using the program SADABS [13], multi-scan absorption corrections were also applied. The structures were solved by a combination of the direct method and the difference Fourier methods provided by the program package SHELXTL [14], and refined using a full matrix least square against F^2 for all data. All the non-H atoms were refined anisotropically. All hydrogen atoms were included in calculated positions with isotropic thermal parameters 1.2 times those of the attached atoms. Crystallographic data and additional details of data collection and refinement are summarized in Table 1.

NMR titrations

^{1}H NMR titrations were performed at room temperature with TMS as the internal standard. Two stock solutions were prepared by dissolving 10 mg of **L** in 1.0 mL of acetonitrile-d_3 and 20 mg of AgNO$_3$ in 0.10 mL of acetonitrile-d_3, respectively. A small portion of the AgNO$_3$ stock solution was added stepwise to the **L** solution in the NMR tube with a Hamilton micro-syringe.

Results and discussion

Synthesis of **L**

An improved procedure for a mercaptan-halide coupling reaction [15] under high-dilution conditions gave a fair yield (ca 37%) of **L**. A molecular ion at *m/z* 284 in its mass spectrum together with elemental analysis data clearly supports the structure of **L**. The aromatic protons of **L** are well resolved as two AA′BB′ systems.

Crystal structure of **L**

The molecular conformation of macrocycles can be specified in terms of the donor atom orientation and torsion angles associated with donor atoms. Molecular mechanics calculations on the thiaoxa macrocycles suggest that lower energy conformations are obtained when O atoms are oriented in an *endodentate* fashion, while the S atoms are positioned *exodentate*. This orientation tendency also has been observed crystallographically in the thiaoxa macrocycles [16, 17].

Table 1. Crystal data and structure refinement for **L**, **1**, and **2**

	L	**1**	**2**
Formula	$C_{14}H_{20}O_2S_2$	$C_{14}H_{20}AgNO_5S_2$	$C_{14}H_{20}Cl_2O_2PtS_2$
M	284.42	454.30	550.41
T, K	293(2)	298(2	298(2)
Crystal system	Monoclinic	Monoclinic	Monoclinic
space group	$C2/c$	$P2_1$	$P2_1/c$
a/Å	14.491(11)	7.3032(4)	8.1736(5)
b/Å	12.104(5)	14.4333(9)	14.3853(10)
c/Å	7.873(5)	7.7457(5)	14.9014(10)
β/°	95.52(7)	102.898(1)	99.4930(10)
V/Å^3	1469.3(15)	851.01(9)	1728.1(2)
Z	4	2	4
D_c/g cm^{-1}	1.286	1.773	2.116
μ/mm^{-1}	0.355	1.452	8.670
$F(000)$	608	460	1056
Crystal size, mm	$0.20 \times 0.30 \times 0.40$	$0.25 \times 0.25 \times 0.50$	$0.10 \times 0.20 \times 0.30$
Theta range for data collection, deg	2.14 to 32.20	2.70 to 28.29	1.98 to 28.27
Limiting indices	$-14 \leqq h \leqq 23$	$-9 \leqq h \leqq 9$	$-10 \leqq h \leqq 8$
	$-17 \leqq k \leqq 17$	$-18 \leqq k \leqq 19$	$-18 \leqq k \leqq 18$
	$-11 \leqq l \leqq 11$	$-10 \leqq l \leqq 4$	$-14 \leqq l \leqq 13$
Reflections collected	6271	5388	10985
Independent reflections	2336 [R_{int} = 0.0453]	3739 [R_{int} = 0.0235]	4073 [R_{int} = 0.0420]
Completeness to theta, %	89.9 (=32.20)	95.1 (=28.29)	95.4 (=28.27)
Absorption correction	None	SADABs[a]	SADABS[a]
Data/restraints/parameters	2336 / 0 / 82	3739 / 1 / 228	4073 / 0 190
GOF on F^2	1.053	1.123	1.034
Final R_1, wR_2			
indices [$I > 2\sigma(I)$]	0.0440, 0.1167	0.0305, 0.0783	0.0418, 0.0114
(all data)	0.0587, 0.1256	0.0313, 0.0790	0.0558, 0.1069
Largest diff. Peak and hole/e Å^{-3}	0.200, −0.399	0.480, −0.607	1.207,[b] −2.712[b]

[a]Reference 13.
[b]Large positive (1.207 e Å^{-3}) and negative (−2.712 e Å^{-3}) difference Fourier peaks are located at short distances from Pt (1.16 and 0.72 Å, respectively). These peaks can be attributed to ghosts of the heavy Pt atom.

An ORTEP drawing of **L** is shown in Figure 1. Atomic coordinates and selected geometric parameters are presented in Tables 2 and 3. **L** has a C_2 axis. As expected the two O atoms are positioned *endodentate* to the ring cavity, while the two S atoms have *exodentate* conformations. The two S atoms in a ring tend to be as far apart as possible [S(1)- - -S(1A); 5.258(4) Å]. As a consequence, they lie at the corner of the pseudo rectangular plane. The aliphatic ring spans *cis* or *gauche* positions between donor atoms [—O—C—C—O—; 20.70(8)° and –O—C—C—S–; 66.70(18)°]. Therefore, the ligand is not well organized to bind a metal ion in a multidentate fashion. A conformational change would be required for the ligand to bind using its S atoms as ligating sites.

Table 2. Atomic coordinates ($\times 10^4$) and equivalent isotropic displacement parameters (Å$^2 \times 10^3$) for **L**

	x/a	y/b	z/c	U_{eq}
S(1)	1660(1)	7343(1)	2053(1)	58(1)
O(1)	901(1)	9721(1)	2812(2)	59(1)
C(1)	441(1)	10671(1)	2184(3)	70(1)
C(2)	1732(1)	9644(2)	2223(2)	66(1)
C(3)	2164(1)	8604(2)	2889(2)	62(1)
C(4)	860(1)	7086(1)	3546(2)	44(1)
C(5)	395(1)	6036(1)	3014(2)	37(1)
C(6)	773(1)	5027(1)	3516(2)	46(1)
C(7)	387(1)	4038(1)	3021(2)	53(1)

U_{eq} is defined as one third of the trace of the orthogonalized U_{ij} tensor.

Crystal structure of **1**, [Ag(**L**)(NO$_3$)]

Reaction of AgNO$_3$ with one molar equivalent of **L** in methanol afforded colorless single crystals of the complex suitable for crystallography. The IR spectrum of the complex shows a strong band at 1356 cm^{-1} due to NO$_3^-$ ion in addition to other ligand peaks, which are slightly shifted in position from those of the free ligand and are of lower intensity. The fast atom bombardment (FAB) mass spectrum of the product shows peaks at *m/z* 391 and 393 corresponding to [^{107}Ag(**L**)]$^+$ and [^{109}Ag(**L**)]$^+$, respectively.

Figure 2 shows the crystal structure of complex **1** and the atomic coordinates and selected geometric parameters are listed in Tables 4 and 5. The molecule is partially disordered with the C(13)–C(14) (0.67) and C(13′)–C(14′) (0.33) units occupying two positions. On complexation with Ag(I), the

Table 3. Selected bond lengths (Å), bond angles (°) and torsion angles (°) for **L**

S(1)—C(3)	1.8097(19)	S(1)—C(4)	1.8148(18)
O(1)—C(2)	1.413(2)	O(1)—C(1)	1.416(2)
C(1)—C(1A)	1.499(4)	C(2)—C(3)	1.497(3)
C(4)—C(5)	1.5005(19)		
C(3)—S(1)—C(4)	101.94(8)	C(2)—O(1)—C(1)	112.51(13)
O(1)—C(1)—C(1A)	109.19(13)	O(1)—C(2)—C(3)	109.36(13)
C(2)—C(3)—S(1)	114.79(13)	C(5)—C(4)—S(1)	107.71(9)
C(6)—C(5)—C(4)	119.05(13)	C(5A)—C(5)—C(4)	122.05(8)
O(1)—C(2)—C(3)—S(1)		66.70(18)	
O(1A)—C(1A)—C(1)—O(1)		20.70(8)	
S(1)—C(4)—C(5)—C(6)		82.60(14)	

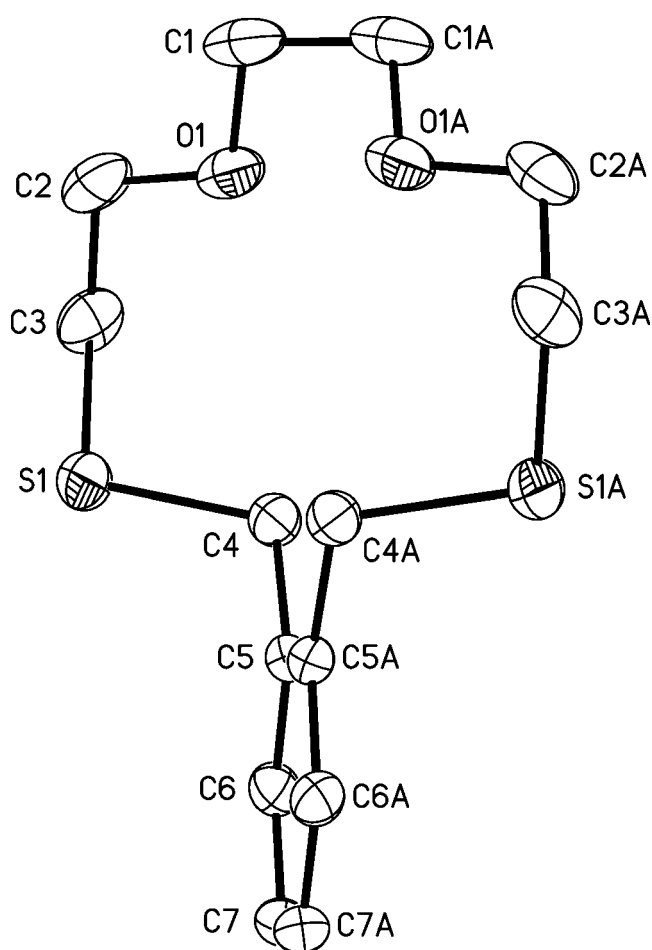Symmetry transformations used to generate equivalent atoms: (A) $-x$, u, $-z + 1/2$.

Figure 1. ORTEP plot of **L** with displacement ellipsoids at the 50% probability level. The H atoms are omitted for clarity.

Table 4. Atomic coordinates ($\times 10^4$) and equivalent isotropic displacement parameters ($\text{Å}^2 \times 10^3$) for **1**, [Ag(**L**)(NO$_3$)]

	x/a	y/b	z/c	U_{eq}
Ag	10043(1)	3170(1)	5861(1)	46(1)
S(1)	10631(2)	4797(1)	6136(1)	42(1)
S(2)	9991(2)	2697(1)	2720(1)	45(1)
O(1)	7178(6)	3869(3)	7037(6)	72(1)
O(2)	6590(5)	2520(3)	4457(5)	72(1)
N(1)	11611(6)	1896(2)	8661(5)	46(1)
O(3)	9988(5)	2204(3)	8302(5)	64(1)
O(4)	12709(7)	2194(4)	7828(8)	103(2)
O(5)	12067(6)	1311(3)	9738(5)	71(1)
C(1)	6922(8)	4748(4)	6535(7)	63(1)
C(2)	8769(7)	5191(3)	7127(7)	56(1)
C(3)	9859(7)	5219(3)	3896(5)	51(1)
C(4)	11259(6)	4990(3)	2787(5)	43(1)
C(5)	12786(7)	5535(3)	2893(7)	56(1)
C(6)	14084(7)	5397(4)	1860(7)	63(1)
C(7)	13882(7)	4696(4)	744(7)	61(1)
C(8)	12384(7)	4130(3)	643(6)	54(1)
C(9)	11034(6)	4272(3)	1653(5)	44(1)
C(10)	9394(7)	3668(3)	1386(6)	49(1)
C(11)	7854(7)	2076(3)	2038(6)	55(1)
C(12)	6151(7)	2438(4)	2598(7)	58(1)
C(13)	5026(12)	3014(10)	4933(13)	61(3)
C(13′)	5330(30)	2593(16)	5590(30)	59(5)
C(14)	5680(10)	3264(9)	6853(11)	63(3)
C(14′)	5160(30)	3535(16)	5690(40)	66(8)

U_{eq} is defined as one of the trace of the orthogonalized U_{ij} tensor.

Table 5. Selected bond lengths (Å), bond angles (°) and torsion angles (°) for **1**, [Ag(**L**)(NO$_3$)]

Ag—O(3)	2.416(4)	Ag—S(2)	2.5326(11)
Ag—S(1)	2.5482(11)	Ag—O(4)	2.657(5)
Ag—O(1)	2.688(4)	Ag—O(2)	2.706(4)
S(1)—C(2)	1.810(5)	S(1)—C(3)	1.820(4)
S(2)—C(11)	1.807(5)	S(2)—C(10)	1.817(5)
O(1)—C(1)	1.412(7)	O(1)—C(14)	1.421(10)
O(1)—C(14′)	1.69(3)	O(2)—C(12)	1.409(6)
O(2)—C(13′)	1.41(2)	O(2)—C(13)	1.487(12)
N(1)—O(5)	1.224(5)	N(1)—O(4)	1.225(6)
N(1)—O(3)	1.249(5)	C(1)—C(2)	1.491(8)
C(3)—C(4)	1.516(6)		
O(3)—Ag—S(2)	125.07(10)	O(3)—Ag—S(1)	125.09(10)
S(2)—Ag—S(1)	109.31(4)		
O(1)—C(1)—C(2)—S(1)		62.3(5)	
O(2)—C(12)—C(11)—S(2)		−57.1(5)	
O(1)—C(14)—C(13)—O(2)		67.3(13)	
O(1)—C(14′)—C(13′)—O(2)		−75.3(20)	

molecular conformation of **L** has been drastically distorted. Thus, all sulfur electron pairs turn from *exo-* to *endodentate* towards the metal-ion center. Additional evidence of the large conformational change of **1** on complexation is the change of the S- - -S distance in the ring for the free ligand [5.258(4) Å] to 4.144(2) Å in complex **1**.

The Ag atom is in a distorted trigonal plane with two coordination sites occupied by the two S atoms of one **L**

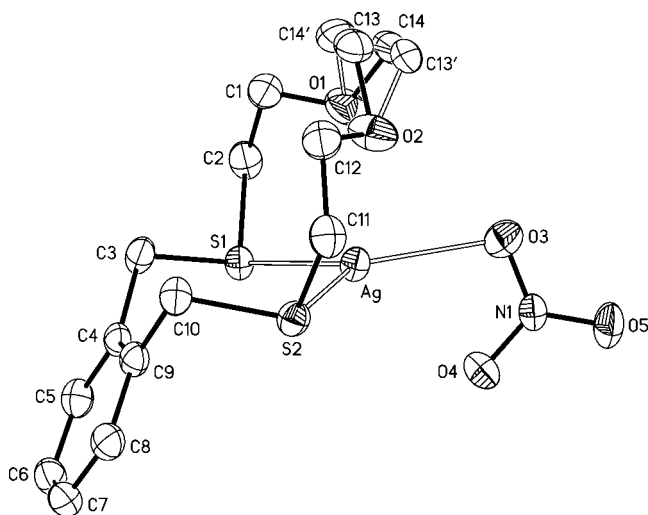*Figure 2.* ORTEP plot of **1** with displacement ellipsoids at the 50% probability level. The H atoms are omitted for clarity.

Figure 3. ^{1}H NMR titration curves for binding of **L** with Ag(I) (as nitrate) in acetonitrile-d_3. For labeling of protons, see formula **L** in this figure.

molecule [Ag—S1; 2.548(1) and Ag—S2; 2.533(1) Å] with an *endodentate* conformation and the third site occupied by one O atom of the NO_3^- ion [Ag—O3; 2.416(4) Å]. To our knowledge, this is the first example of a trigonal Ag(I) complex coordinated by one O atom from a monodentate nitrate ion and two S donor atoms.

The S(1)—Ag—S(2) angle for the seven-membered chelate ring is 109.31(4)° and the O(3)—Ag—S(2) and O(3)—Ag—S(1) angles are 125.07(10) and 125.09(10)°, respectively, giving a Y-shaped geometry. In addition, long-range interaction of the Ag atom with O-donors of a macrocycle and nitrate ion, which are shorter than the sum of Ag and O van der Waals radii (3.20 Å) [18] are observed: [Ag---O(1); 2.688(4), Ag---O(2); 2.707(4) and Ag---O(4); 2.657(5) Å]. The Ag atom is displaced out of the trigonal $S_2(O)$ coordination plane by 0.105(2) Å. The distortion of the trigonal planar geometry of Ag atom could be attributed to the long-range interactions of Ag and O atoms.

^{1}H-NMR titrations were carried out to explore interactions of **L** with Ag(I) in solution for comparison with those in the solid state. The chemical shifts were measured as a function of the mole ratio of Ag(I) to **L** and the titration curves are shown in Figure 3. The titration curves for each proton indicate the initial formation of a 1 : 2 (Ag/**L**) complex which is then converted into a 1 : 1 species as the concentration of Ag(I) in solution increases. The chemical shifts beyond mole ratio = 1 are nearly constant, which suggests that the stoichiometry of this complex is 1 : 1 and the complex is quite stable. The order of magnitude of the chemical shift variation is $H_2 > H_3 > H_1 \geq H_4$, indicating that Ag(I) is strongly coordinated by the S atoms, and the O atom in a ring interacts with the Ag(I) weakly, similar to the case in solid state.

Crystal structure of **2**, *[Pt(**L**)Cl$_2$]*

The reaction of **L** with 1 molar equivalent of K_2PtCl_4 afforded a yellow crystalline product. The fast atom bombardment (FAB) mass spectrum of the product showed a mo-
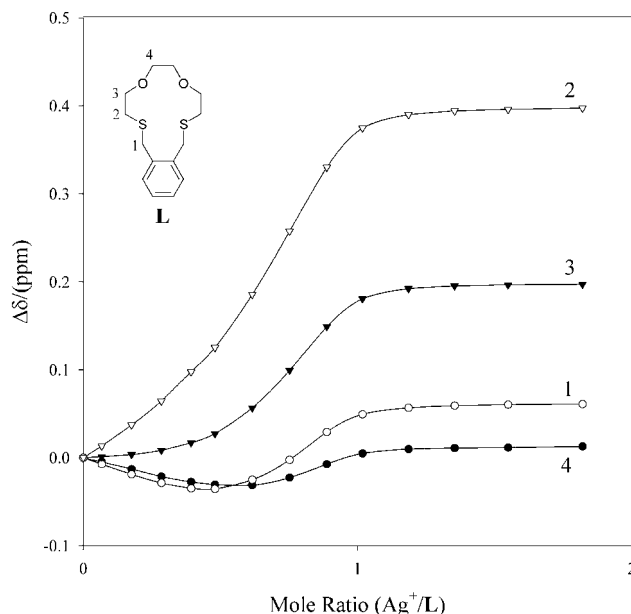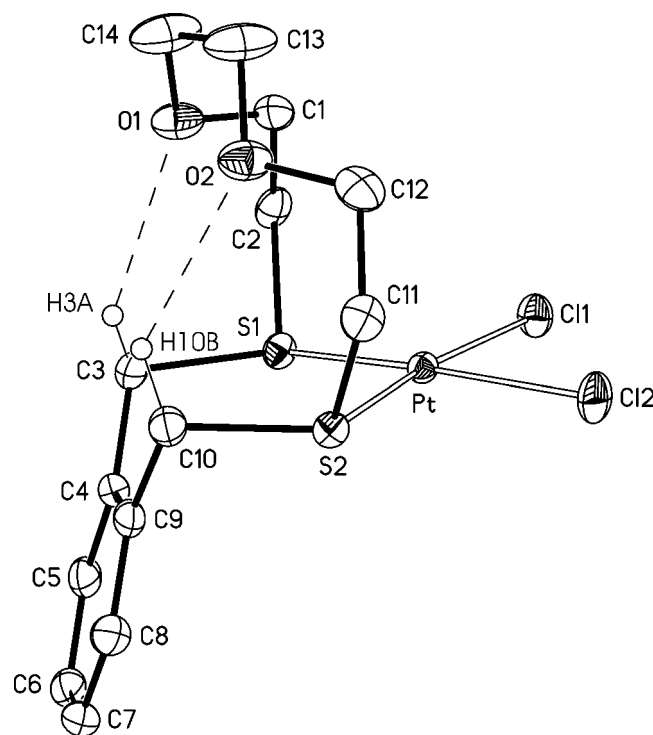

Figure 4. ORTEP plot of **2** with displacement ellipsoids at the 50% probability level. The non-hydrogen bonding H atoms are omitted for clarity.

lecular ion peak at *m/z* 515 corresponding to $[^{195}Pt(\mathbf{L})Cl]^+$. This together with the microanalytical data confirms the formulation as [Pt(**L**)Cl$_2$]. The Pt(II) complex of **L** (Figure 4) is similar in structure to the analogous Pd(II) complex [11]. Atomic coordinates and selected geometric parameters are presented in Tables 6 and 7.

As shown in Figure 5, the Pt atom is four-coordinate in a square-planar environment. It is coordinated to two S atoms of **L** and to two Cl$^-$ ions in a *cis* arrangement. The

Table 6. Atomic coordinates ($\times 10^4$) and equivalent isotropic displacement parameters ($\text{Å}^2 \times 10^3$) for **2**, [Pt(**L**)Cl$_2$]

	x/a	y/b	z/c	U_{eq}
Pt	7830(1)	459(1)	2127(1)	32(1)
Cl(1)	9664(2)	941(1)	1190(1)	50(1)
Cl(2)	6613(3)	1921(1)	1962(2)	59(1)
S(1)	9458(2)	−840(1)	2277(1)	39(1)
S(2)	5894(2)	204(1)	3045(1)	39(1)
O(1)	6696(7)	−2087(4)	1099(4)	62(2)
O(2)	3984(8)	−1103(5)	1506(4)	65(2)
C(1)	7672(11)	−1528(6)	627(5)	57(2)
C(2)	9363(10)	−1395(5)	1183(5)	50(2)
C(3)	8817(10)	−1800(5)	2943(5)	50(2)
C(4)	8833(10)	−1503(5)	3904(5)	43(2)
C(5)	10264(10)	−1581(5)	4549(6)	53(2)
C(6)	10338(11)	−1317(5)	5426(6)	56(2)
C(7)	8950(13)	−951(6)	5694(6)	67(3)
C(8)	7497(11)	−854(6)	5077(6)	58(2)
C(9)	7427(10)	−1118(5)	4171(5)	48(2)
C(10)	5861(9)	−971(5)	3503(5)	49(2)
C(11)	3862(10)	274(6)	2337(6)	54(2)
C(12)	3702(10)	−160(7)	1418(6)	62(2)
C(13)	3896(12)	−1539(9)	648(8)	93(4)
C(14)	5039(12)	−2263(9)	661(8)	95(4)

U_{eq} is defined as one third of the trace of the orthogonalized U_{ij} tensor.

Table 7. Selected bond lengths (Å), bond angles (°) and torsion angles (°) for **2**, [Pt(**L**)Cl$_2$]

Pt—S(1)	2.2836(16)	Pt—S(2)	2.2858(18)
Pt—Cl(1)	2.3168(18)	Pt—Cl(2)	2.3209(17)
S(1)—C(2)	1.806(7)	S(1)—C(3)	1.827(8)
S(2)—C(11)	1.818(8)	S(2)—C(10)	1.825(8)
O(1)—C(1)	1.401(10)	O(1)—C(14)	1.425(10)
O(2)—C(12)	1.378(11)	O(2)—C(13)	1.415(11)
C(1)—C(2)	1.502(11)	C(3)—C(4)	1.493(10)
S(1)—Pt—S(2)	105.05(6)	S(1)—Pt—Cl(1)	83.05(7)
S(2)—Pt—Cl(2)	83.24(7)	Cl(1)—Pt—Cl(2)	88.51(7)
O(1)—C(14)—C(13)—O(2)	−46.1(6)		
O(1)—C(1)—C(2)—S(1)	60.5(8)		
O(2)—C(12)—C(11)—S(2)	63.1(8)		

Table 8. Hydrogen-bonding geometry (Å, °) for **2**, [Pt(**L**)Cl$_2$]

D-H- - -A	D-H	H- - -A	D- - -A	D-H- - -A
C3-H3A- - -O1	0.96	2.371	3.0245(99)	125.0
C10-H10B- - -O2	0.96	2.525	3.1210(97)	120.3

believed to result from the conformational steric demand of the bicyclic rings consisting of seven- and eleven membered rings formed by the chelating of Pt(II) to two S atoms.

References

1. R.M. Izatt, G. Wu, W. Jiang and N.K. Dalley: *Inorg. Chem.* **29**, 3828 (1990).
2. A.J. Blake, G. Reid and M. Schröder: *J. Chem. Soc., Chem. Commun.* 1074 (1992).
3. Y.-H. Lai, L. Ma and K.F. Mok: *New J. Chem.* **21**, 985 (1997).
4. W. Liang, S. Liu, C.R. Lucas and D.O. Miller: *Polyhedron* **17**, 1323 (1998).
5. J.W. Silbert, S.J. Lange, D.J. Williams, A.G.M. Barrett and B.M. Hoffman: *Inorg. Chem.* **34**, 2300 (1995).
6. J. Casabó, F. Teixidor, L. Escriche, C. Viñas and C. Pérez-Jiménez: *Adv. Mater.* **7**, 238 (1995) and the references therein.
7. M. Oue, K. Akama, K. Kimura, M. Tanaka and T. Sono: *J. Chem. Soc., Perkin Trans. I* 1675 (1989).
8. M.-T. Lai and J.-S. Shih: *Analyst* **111**, 891 (1986).
9. Y.H. Lee and S.S. Lee: *J. Incl. Phenom.* **39**, 235 (2001).
10. B.L. Lee, Y.H. Lee, I. Yoon, J.H. Jung, K.-M. Park and S.S. Lee: *Microchem. J.* **68**, 241 (2001).
11. I. Yoon, B.S. Yoo, S.S. Lee and B.G. Kim: *Acta Crystallogr.* **C56**, 758 (2000).
12. K.-M. Park, I. Yoon, B.S. Yoo, J.B. Choi, S.S. Lee and B.G. Kim: *Acta Crystallogr.* **C56**, 1191 (2000).
13. Siemens: *Area Detector Control and Integration Software*. Version 4.0. in SMART and SAINT, Siemens Analytical X-ray Instruments Inc., Madison, Wisconsin (1996).
14. Siemens: *Structure Determination Programs*. Version 5.03, in SHELXTL. Siemens Analytical X-ray Instruments Inc., Madison, Wisconsin (1996).
15. J. Buter and R.M. Kellog: *J. Chem. Soc., Chem. Commun.* 466 (1980).
16. N.K. Dalley, J.S. Smith, S.B. Larson, K.L. Matheson, J.J. Christensen and R.M. Izatt: *J. Chem. Soc., Chem. Commun.* **84** (1975).
17. G.J. Grant, D.F. Galas, M.W. Jones, K.D. Loveday, W.T. Pennington, G.L. Schimek, C.T. Eagle and D.G. VanDerveer: *Inorg. Chem.* **37**, 5299 (1998).
18. A.F. Wells, *Structural Inorganic Chemistry*, Oxford University Press, Oxford (1984).
19. H.-J. Drexler: Thesis, University of Rostock (1997).
20. A.A. Dvorkin, Y.A. Simonov, T.I. Malinovskii, S.V. Pavlova and L.I. Budarin: *Zh. Neorg. Khim.* **34**, 2593 (1989).
21. R. Taylor and O. Kennard: *J. Am. Chem. Soc.* **104**, 5063 (1982).

two Pt-S bond lengths in the complex average 2.285(2) Å, comparable to other Pt(II) complexes of thia or thiaoxa macrocycles [2.226–2.286 Å] [19, 20]. In the complex, the two O atoms lie *cis* to each other and are oriented away from the Pt center, precluding Pt-O interaction. The benzylic C(3) and C(10) atoms are positioned on the same side of the two O atoms and there is a pair of C—H- - -O hydrogen-bonding interactions [21] between C(3) and O(1) [3.025(10) Å] and C(10) and C(2) [3.121(10) Å]. Their parameters are given in Table 8.

It is noted that the S—Pt—S bond angle of 105.05(6)° is significantly larger than the Cl—Pt—Cl bond angle of 88.51(7)°. The large difference in the two bond angles is